Mixed convection flow of nanofluid in a square enclosure with an intruded rectangular fin

Ran Cong, Xuanyu Zhou, Bruno De Souza Machado, and Prodip K. Das

Citation: AIP Conference Proceedings **1754**, 050017 (2016); doi: 10.1063/1.4958408
View online: http://dx.doi.org/10.1063/1.4958408
View Table of Contents: http://scitation.aip.org/content/aip/proceeding/aipcp/1754?ver=pdfcov
Published by the AIP Publishing

Mixed Convection Flow of Nanofluid in a Square Enclosure with an Intruded Rectangular Fin

Ran Cong, Xuanyu Zhou, Bruno De Souza Machado, Prodip K. Das [a)]

School of Mechanical and Systems Engineering
Newcastle University
Newcastle upon Tyne, NE1 7RU
United Kingdom

[a)]Corresponding author: prodip.das@ncl.ac.uk

Abstract. Mixed convection flow in enclosures has been a subject of interest for many years due to their ever increasing applications in solar collectors, electronic cooling, lubrication technologies, food processing, and nuclear reactors. In comparison, little effort has been given to the problem of mixed convection in enclosures filled with nanofluids, while the addition of nanoparticles in a fluid base to alter specific material properties is considered a feasible solution for many heat transfer problems. Mixed convection of nanofluids is a challenging problem as the addition of nanoparticles changes the fluid's thermo-physical properties as well as due to the complex interactions among inertia, viscous, and buoyancy forces. In this study, a two-dimensional steady-state numerical model has been developed to investigate mixed convection flow of nanofluids in a square enclosure with an intruded rectangular fin and to optimize the fin geometry for maximizing the heat transfer using the Constructal design. The model has been developed using ANSYS-FLUENT for various fin geometries. Flow fields, temperature fields, and heat transfer rates are examined for different values of Rayleigh and Reynolds numbers for several geometries of the fin with the aim of maximizing the heat transfer from the fin to the surrounding flow. Outcome of this study provides important insight into the heat transfer behavior of nanofluids, which will help in developing novel geometries with enhanced and controlled heat transfer for solar collectors and electronic devices.

Keywords: Mixed convection, Nanofluids, Numerical modeling, Rectangular fin, Constructal design.

INTRODUCTION

The study of convective heat transfer inside cavities, such as triangular, trapezoidal, cylindrical, square, wavy, etc. [1-6], has been extensively analyzed due to their application in several engineering problems such as solar collectors, electronic cooling, lubrication technologies, food processing, nuclear reactors, and cooling gas turbine components via internal convective flows. These studies were essential to provide a better understanding of the physics regarding the fluid dynamics and heat transfer inside the cavities as well as for thermal enhancement and optimization. By narrowing the cavity design to a square lid driven cavity, many studies were carried out for both laminar and turbulent conditions. Nevertheless, due to the equipment miniaturization trend, easily noticed in electronic devices, the technical challenge of increasing the heat transfer inside the cavity without changing the cavity area still remained. Researchers proposed the addition of different types of fin in the cavity and filled with nanofluids, which is the combination of a fluid-base and nanoparticles to enhance certain desired property, in order to increase the heat transfer inside the cavity [7-9].

International Conference on Mechanical Engineering
AIP Conf. Proc. 1754, 050017-1–050017-8; doi: 10.1063/1.4958408
Published by AIP Publishing. 978-0-7354-1412-9/$30.00

A large number of experimental and numerical works has been performed for the geometrical optimization of fins and cavities using the Constructal design [7-11]. The Constructal design is based on the Constructal law, which was stated by Adrian Bejan as "For a finite-size system to persist in time (to live), it must evolve in such a way that it provides easier access to the imposed currents that flow through it" [12]. The Constructal law accounts for the universal phenomenon of generation and evolution of design (configuration, shape, structure, pattern, rhythm). It has guided researches toward the discovery of efficient cooling structures for various cavities. However, previous Constructal design studies are primarily based on air or water filled cavities. It has not been employed to the geometrical optimization of fins and cavities filled with nanofluids. Therefore, the main purpose of this study is to investigate the geometrical optimization of fins and cavities filled with nanofluids by means of the Constructal design concept. In the present study, a two-dimensional steady-state numerical model has been developed to investigate mixed convection flow of nanofluids in a square enclosure with an intruded rectangular fin and to optimize the fin geometry for maximizing the heat transfer. The Constructal design method is used to obtain the optimum geometry, in other words, the one that has the maximum heat transfer between the nanofluid and fin. The fin area and the aspect ratio of fin's height and length are considered the degrees of freedom of the finite flux system. For these degrees of freedom, several values of Rayleigh (Ra) and Reynolds (Re) numbers are considered. For the selected problem, a nanofluid resulted by the mixture of water and 1% of aluminum oxide (Al_2O_3) is utilized. For all the simulations, the Prandtl number (Pr) is kept fixed as Pr = 6.6 for 1% Al_2O_3-water nanofluid.

MATHEMATICAL AND NUMERICAL MODELING

The governing equations for the laminar, two-dimensional, steady state mixed convection fluid flow and heat transfer with the Boussinesq approximation in y-direction are written as:

$$\frac{\partial u}{\partial x}+\frac{\partial v}{\partial y}=0 \tag{1}$$

$$u\frac{\partial u}{\partial x}+v\frac{\partial u}{\partial y}=-\frac{1}{\rho_{nf}}\frac{\partial p}{\partial x}+\frac{\mu_{nf}}{\rho_{nf}}\left(\frac{\partial^2 u}{\partial x^2}+\frac{\partial^2 u}{\partial y^2}\right) \tag{2}$$

$$u\frac{\partial v}{\partial x}+v\frac{\partial v}{\partial y}=-\frac{1}{\rho_{nf}}\frac{\partial p}{\partial y}+\frac{\mu_{nf}}{\rho_{nf}}\left(\frac{\partial^2 v}{\partial x^2}+\frac{\partial^2 v}{\partial y^2}\right)+\frac{(\rho\beta)_{nf}}{\rho_{nf}}g\left(T-T_\infty\right) \tag{3}$$

$$u\frac{\partial T}{\partial x}+v\frac{\partial T}{\partial y}=\frac{k_{nf}}{(\rho C_p)_{nf}}\left(\frac{\partial^2 T}{\partial x^2}+\frac{\partial^2 T}{\partial y^2}\right) \tag{4}$$

where u and v are the horizontal and vertical velocities, p is the thermodynamic pressure, μ_{nf} is the effective dynamic viscosity, ρ_{nf} is the effective density, β_{nf} is the thermal expansion coefficient, T is the temperature, g is the standard gravity, k_{nf} is the heat conductivity, and $C_{p,nf}$ is the heat capacity. The subscript nf represents the effective nanofluid properties, which are computed based on the volume fraction of nanoparticles (φ) in the base fluid. The viscous dissipation term in the energy equation is neglected assuming the heat due to friction between the nanoparticles and fluid is negligible compared to conduction at the heated surface. The effective dynamic viscosity of the nanofluid is calculated according to the Brinkman model [13] and the effective thermal conductivity is determined using the Maxwell model [14-16]. Following equations are used to compute the nanofluid properties:

$$\rho_{nf}=(1-\varphi)\rho_f+\varphi\rho_s \tag{5}$$

$$\mu_{nf} = \frac{\mu_f}{(1-\varphi)^{2.5}} \tag{6}$$

$$k_{nf} = k_f \frac{k_s + 2k_f - 2\varphi(k_f - k_s)}{k_s + 2k_f + \varphi(k_f - k_s)} \tag{7}$$

$$(\rho C_p)_{nf} = (1-\varphi)(\rho C_p)_f + \varphi(\rho C_p)_s \tag{8}$$

$$(\rho\beta)_{nf} = (1-\varphi)(\rho\beta)_f + \varphi(\rho\beta)_s \tag{9}$$

where the subscript *s* and *f* represent the solid nanoparticle and base-fluid properties, respectively. It is assumed that base-fluid (in this case water) and nanoparticles (Al_2O_3) are in thermal equilibrium, and nanofluid's thermo-physical properties are constant. Thermo-physical properties of water, Al_2O_3 nanoparticles, and Al_2O_3-water nanofluid (volume fraction of the nanoparticles, φ, is 1%) are listed in Table 1.

TABLE 1. Thermo-physical properties of base-fluid, nanoparticles, and nanofluid.

Physical properties	**Base fluid (water)**	**Nanoparticles (Al_2O_3)**	**Nanofluid**
C_p [J/(kg·K)]	4179	765	4047.01
ρ [kg/m^3]	997.1	3970	1026.83
k [W/m·K]	0.613	40	0.63074
β [1/K]	2.1×10^{-4}	8.5×10^{-6}	2.02×10^{-4}
μ [kg/m]	1.002×10^{-3}	-	1.03×10^{-3}

The numerical solution is obtained by solving the governing equations using commercial finite volume based software, ANSYS-FLUENT. A second order upwind scheme is used for the spatial discretization of the aforementioned equations. Further, the velocity-pressure coupling is done by the SIMPLE algorithm and pressure based solver is used to compute the solution. The solution of governing equations is considered converged when the residuals are smaller than 10^{-7} for mass and momentum equation and smaller than 10^{-8} for energy equation. The numerical simulations are performed using a desktop computer with a quad-core Intel processor with 2.67 GHz clock and 32GB of RAM. In order to select a mesh in which the error associated does not affect significantly the results, a mesh independence test is carried out by comparing the mean Nusselt number between the fin and top wall for various meshes. The results of a mesh independency test are given in Table 2 for mesh densities of 100×100, 120×120, and 160×160 for Ra = 10^5 and φ = 1%. All three meshes produce numerical results that are less than 2% in error, while error in 120×120 mesh is less than 1%. Therefore, the 120×120 volumes mesh is considered to perform the simulations.

TABLE 2. Values of mean Nusselt number for different mesh densities.

Volumes	**Mean Nusselt number**	**% Error**
10000	11.017	1.743
14400	11.106	0.801
25600	11.177	0.638

PROBLEM DESCRIPTION

The selected problem considers a lid-driven square cavity with a fin intruded in its bottom center as shown in Figure 1. The top surface of the cavity moves through the x axis direction and a constant temperature (T_{min}) is defined at it. However, the fin surface has a constant wall temperature (T_{max}) boundary condition. In Figure 1, H and L are the height and length of the cavity, H_1 and L_1 are the height and length of the fin, and A and A_f are the areas of the cavity and the fin, respectively. All exterior surfaces but the top surface are considered adiabatic and no slip condition is valid. The dimensionless velocities (u^* and v^*) and temperature (θ) in Figure 1 are defined as

$$u^* = \frac{u}{u_{max}},\ v^* = \frac{v}{u_{max}},\ \text{and}\ \theta = \frac{T - T_{min}}{T_{max} - T_{min}} \tag{10}$$

The area of the cavity is kept fixed as $A = 1$ m^2 and different fin areas are tested. The relation of cavity and fin areas is represented by the area fraction of the fin, ϕ, which is the ratio between the fin and cavity areas. In this study, three different values of ϕ are considered: 0.05, 0.10 and 0.15. A set of non-dimensional numbers are used to modify the relation between buoyancy and inertial forces. The Reynolds (Re), Rayleigh (Ra), Prandtl (Pr), and Richardson number (Ri), which are defined as

$$\mathrm{Re} = \frac{\rho_{nf} u_{max} H}{\mu_{nf}},\ \mathrm{Ra} = \frac{g\beta_{nf}\Delta T L^3}{\nu_{nf}\alpha_{nf}},\ \mathrm{Pr} = \frac{\nu_{nf}}{\alpha_{nf}},\ \text{and}\ \mathrm{Ri} = \frac{\mathrm{Ra}}{\mathrm{PrRe}^2} \tag{11}$$

where α is the thermal diffusivity and ν is the kinematic viscosity. For different buoyancy forces considered in this study, the Rayleigh numbers are varied between 10^3 and 10^8. For different inertial forces, the Reynolds numbers are varied between 100 and 2000. Finally, the averaged Nusselt number (Nu_{avg}) is calculated through the integral of the local Nusselt number (Nu_L) over the fin surface.

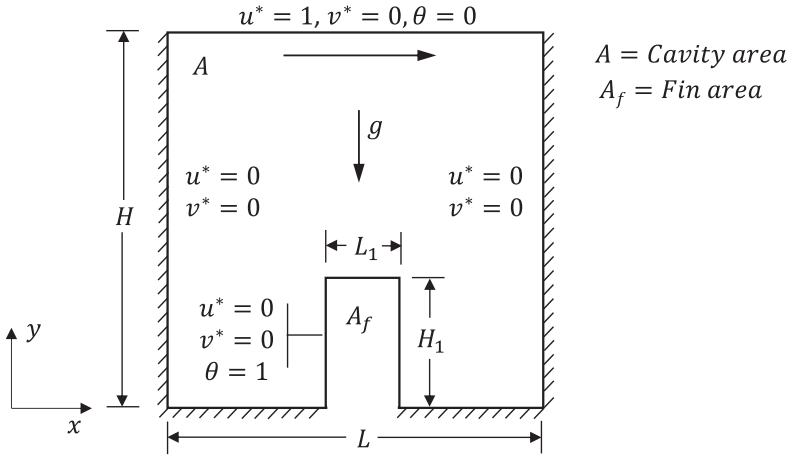

FIGURE 1. Schematic diagram of the cavity flow domain.

RESULTS AND DISCUSSION

In this section, numerical results of mixed convection fluid flow and heat transfer of the Al_2O_3-water nanofluid in a lid-driven square cavity with an intruded rectangular fin are presented. Firstly, the numerical method is evaluated by means of a comparison with other results of literature. A simulation of a convective flow in a partially heated rectangular enclosure filled with a nanofluid is performed. Here a simplified geometry is considered with the omission of intruded fin, which is identical to the geometry used by Oztop and Abu-Nada [17]. This geometry

considers a heater on the left wall, which is half the size of wall height and maintained at a constant temperature (T_{max}) higher than the right wall (T_{min}). The top and bottom walls of the enclosure are considered insulated. Figure 2 shows a comparison between present numerical results with the results presented by Oztop and Abu-Nada for different Rayleigh numbers. Here averaged Nusselt number (Nu_{avg}) is estimated by integrating local Nusselt number over the heater surface. It is quite clear that present numerical results for a partially heated rectangular enclosure are in good agreement with the results available in literature [17].

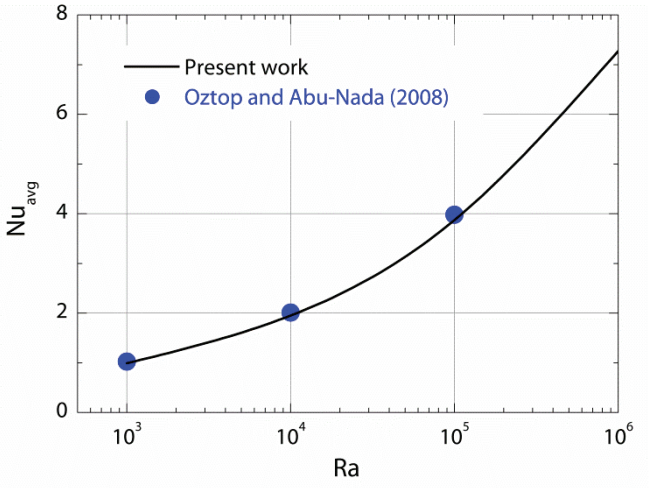

FIGURE 2. Averaged Nusselt number (Nu_{avg}) versus Rayleigh number (Ra) and a comparison with published data.

Effects of Reynolds and Rayleigh Numbers

The influences of Reynolds and Rayleigh numbers on the heat transfer between the fin and nanofluid are shown in Figure 3. Here Figure 3a shows the effects of Reynolds numbers on the averaged Nusselt number (Nu_{avg}) as a function of fin aspect ratio (H_1/L_1) for the area fraction of 0.05 and Ra = 10^5. It is observed that as the fin aspect ratio increases from 0.1, heat transfer from the fin increases and it reaches at a maximum point and then decreases. Figure 3a reveals that higher Reynolds numbers provide higher heat transfer from the fin to the nanofluid. However, the trend remains the same for all Reynolds numbers primarily due to the forced convection, which can be verified by Figure 3b as it shows the forced, mixed, and natural convection regimes as a function of Richardson, Reynolds, and Rayleigh numbers for 1% Al_2O_3-water nanofluid. As observed in Figure 3b, the heat transfer regime for Ra = 10^5 and 500 < Re < 2000 is predominantly the forced convection as the Richardson number remains below 0.1. Figure 3a further reveals that the shape $H_1/L_1 = 0.1$ has a better heat transfer performance than the shape $H_1/L_1 = 10$ for all Reynolds numbers. For instance, at Re = 1000, the best shape for this case is obtained for an intermediate ratio of $(H_1/L_1)_{opt} = 0.46$. For the optimal shape, it is obtained a $Nu_{avg} = 24.5$ which is nearly 32% and 110% higher than that obtained for the lowest and highest ratios of H_1/L_1, $H_1/L_1 = 0.1$ and $H_1/L_1 = 10$, respectively. Clearly, the increase of superficial area (at $H_1/L_1 = 10$) does not necessarily leads to an increase of heat transfer rate from the fin to the fluid flow. This heat transfer pattern indicates the importance of Constructal design for optimization of convective flows problems.

The effects of Rayleigh numbers on the averaged Nusselt number for the optimum fin aspect ratio, $(H_1/L_1)_{opt}$, for the area fraction of the fin of 0.05 are shown in Figure 3c. The averaged Nusselt number for the optimum fin aspect ratio is denoted as $Nu_{avg,max}$. Although increasing Reynolds number increases $Nu_{avg,max}$, the effects of Rayleigh number on $Nu_{avg,max}$ are negligible for the entire range of Reynolds numbers (100 to 2000) for Ra ≤ 10^5. Even for a high Rayleigh number (Ra = 10^6), change in $Nu_{avg,max}$ is small at high Reynolds number (for Re > 1000). This can be further explained by examining Figure 3b, as it shows that at Re = 1000, changing Rayleigh number from 10^3 to 10^6 does not change the heat transfer regime. For all four cases of Rayleigh number, fluid motion is dominated by the forced convection. Conversely, for low Reynolds number (Re < 500), $Nu_{avg,max}$ increases with Rayleigh numbers as

the fluid motion at high Rayleigh numbers is dominated by the mixed convection ($0.1 < Ri < 10$). For low Re, one can also increase the Richardson number over 0.1 by increasing Rayleigh number, which will shift the heat transfer regime from the forced to mixed convection and then to free convection, as shown in Figure 3d where $Nu_{avg,max}$ values are shown for several higher Rayleigh numbers ($Ra > 10^6$). As observed, $Nu_{avg,max}$ increases with Richardson numbers, i.e. with Rayleigh numbers. Here heat transfer from fin's side walls increases as the buoyancy force increases with Rayleigh numbers due to the mixed convection. Clearly, the increase of Rayleigh number can also be effective in the maximization of the heat transfer for low Reynolds numbers ($Re \leq 100$) due the buoyancy force dominance in the flow. When comparing the cases for $Ra = 10^3$ to $Ra = 10^5$ for $Re = 100$, the increase in the heat transfer is over 20% as observed in Figure 3c.

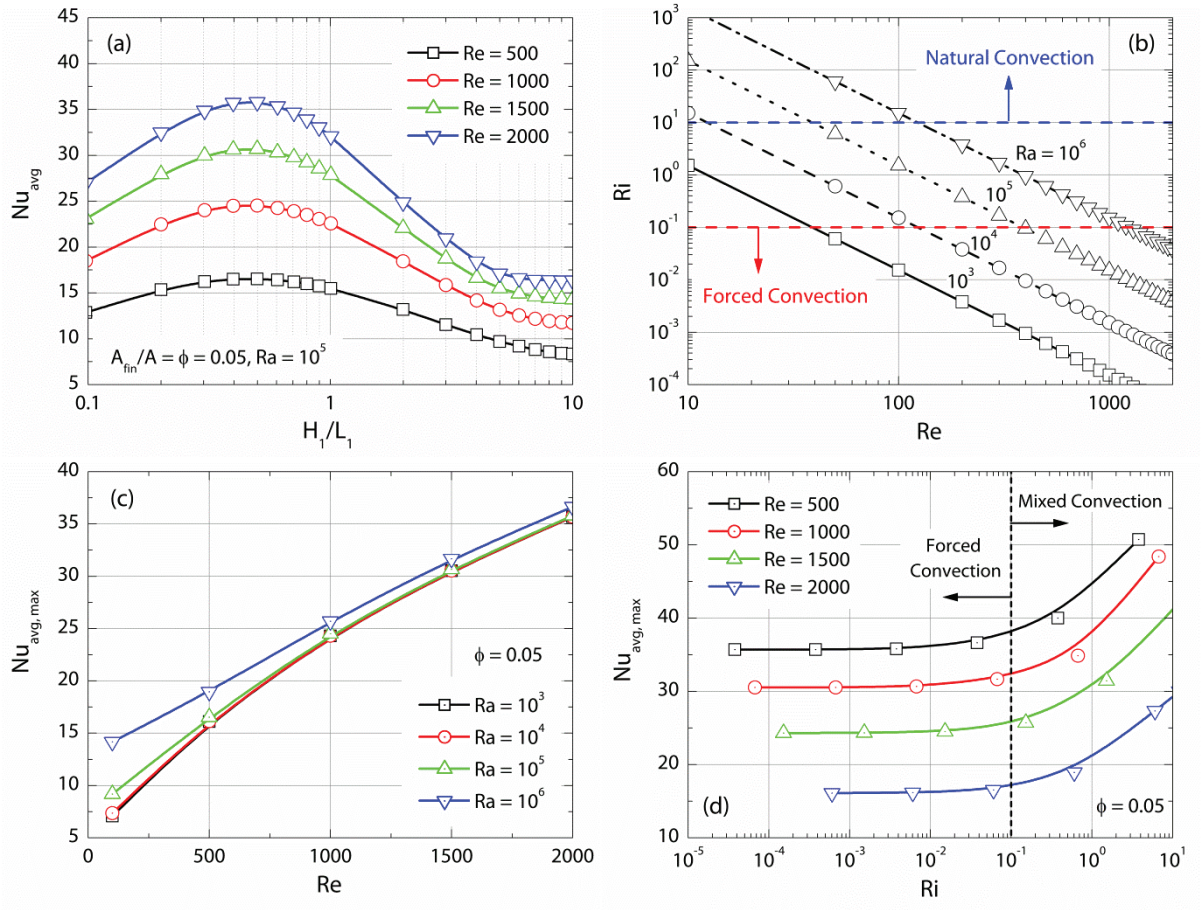

FIGURE 3. Influences of Reynolds and Rayleigh numbers: (a) Effect of fin aspect ratio (H_1/L_1) on Nu_{avg} for various Reynolds numbers at $\phi = 0.05$, (b) Richardson number as a function of Reynolds number for various Rayleigh numbers for Al_2O_3-water nanofluid, (c) Effect of Rayleigh numbers on averaged Nusselt number for the optimum fin aspect ratio, and (d) Effect of Richardson numbers on averaged Nusselt number for the optimum fin aspect ratio ($(H_1/L_1)_{opt}$).

Effect of Fin Aspect Ratio

The optimum fin aspect ratio is the one that maximizes the heat transfer between the fin and nanofluid. No great variation in the optimum fin aspect ratio is observed for the area fraction of the fin of 0.05 for $Ra < 10^5$, as presented in Figure 4a as a function of Reynolds number. The optimum aspect ratio stands approximately at $(H_1/L_1)_{opt} = 0.46$ for all Rayleigh numbers when $Re \leq 1000$. The increase of the aspect ratio creates recirculation zones in the corner of the cavity, decreasing the heat transfer between the fin and nanofluid. For higher Reynolds number ($Re > 1000$), the optimum aspect ratio decreases slightly, which indicates that a wider fin will have better heat transfer than a

taller fin. This is primarily due to forced convection (as illustrated in Figure 3b for $Ra < 10^5$ and $500 < Re < 2000$) as a taller fin will provide higher flow resistance in the cavity and fluid mixing will be interrupted. For higher Rayleigh number ($\geq 10^7$), the optimum fin aspect ratio increases with Reynolds numbers as the heat transfer process is shifting toward the mixed convection regime (see Figure 3b). A close look to the case of Re = 1000, as illustrated in Figure 4b, depicts that the optimum fin aspect ratio increases at high Rayleigh number ($\geq 10^7$) due to the mixed convection. It indicates that the optimum fin aspect ratio is independent of Rayleigh and Reynolds numbers in the forced convection regime, while it is strongly influenced by Rayleigh and Reynolds numbers in the mixed convection regime. By the means of Constructal design method, the optimum fin aspect ratio for $\phi = 0.05$ is found to be 0.46 for the selected set of degrees of freedom and constrains of $Re < 1000$ and $10^3 \leq Ra \leq 10^5$. For $Ra = 10^7$, the optimum fin aspect ratio is found to be between 0.46 and 0.56 for $\phi = 0.05$ as shown in Figure 4a.

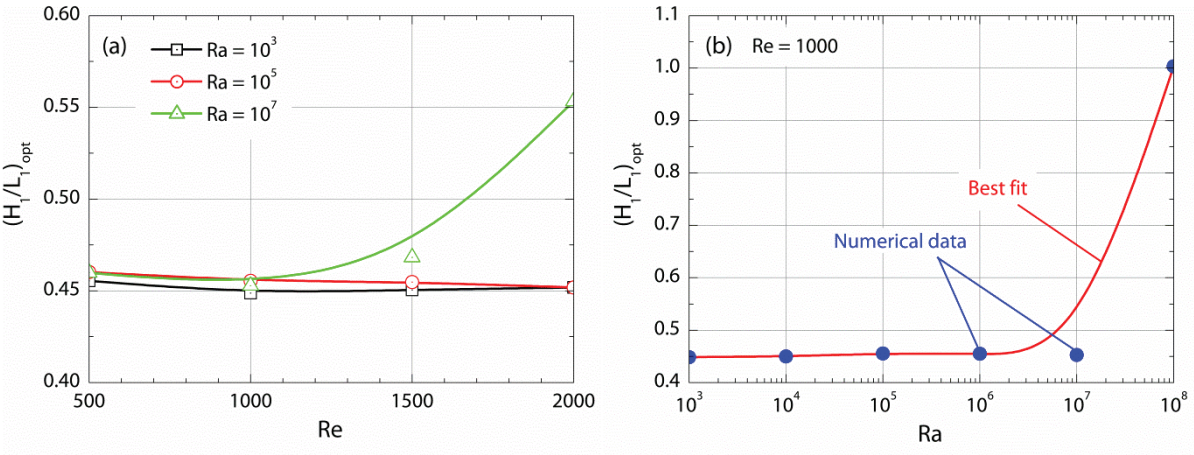

FIGURE 4. Optimum fin dimension as a function of (a) Reynolds number and (b) Rayleigh number for the area fraction of the fin of $\phi = 0.05$.

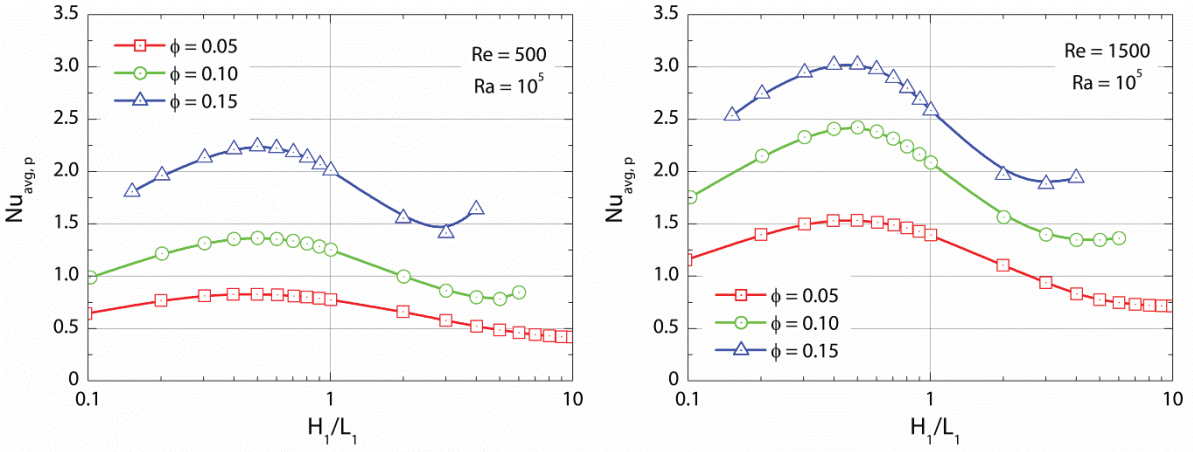

FIGURE 5. Effect of the area fraction of the fin on the spatial-averaged Nusselt number ($Nu_{avg,p}$) for different Reynolds numbers.

Effect of Area Fraction of the Fin

The size of the fin with respect to the cavity will have an impact on overall heat transfer process. A larger fin may provide higher heat transfer for a fixed temperature gradient due to higher surface area. However, a lager fin may introduce a larger flow resistance due to larger area inside the cavity. Hence, it is important to see how the area

fraction of the fin (ϕ) affects the heat transfer. The fin influence on $Nu_{avg,p}$ has been evaluated for two Raynolds numbers as depicted in Figure 5. Since the fin's perimeter changes with the area ratio, a special characteristic length is used here to estimate the spatial-averaged Nusselt number ($Nu_{avg,p}$). The characteristic parameter (p) is estimated by dividing the fin area with the cavity height. It is observed from Figure 5, the qualitative nature of $Nu_{avg,p}$ as a function of fin aspect ratio is almost identical for both Reynolds numbers. $Nu_{avg,p}$ increases with the fin aspect ratio and after the optimum the fin aspect ratio, $Nu_{avg,p}$ decreases for all the area fraction of the fin and for all these area fractions the optimum aspect ratio of the fin remains almost identical.

CONCLUSIONS

A numerical study has been performed to investigate the mixed convection flow of an Al_2O_3-water nanofluid in a square lid-driven cavity with an intruded rectangular fin and to optimize the fin geometry for maximizing the heat transfer using the Constructal design concept. Some important conclusions can be drawn from the obtained results, such as

- The resistance to the flow caused by the different aspect ratio and also the different area ratio have a big influence in the heat transfer inside the cavity;
- The buoyancy force only presents an effective influence in the heat transfer for high values Rayleigh number, where the convective flow becomes a mixed convection dominant flow;
- The variation of the Rayleigh and Reynolds numbers did not affect significantly the ranging of fin's optimum aspect ratio
- The optimum fin aspect ratio for $\phi = 0.05$ is found to be 0.46 for $Re < 1000$ and $Ra \leq 10^7$and for $Re > 1000$ and $Ra \geq 10^7$, the optimum fin aspect ratio is found to be within 0.46 and 0.56.

In the future, this study can be extended for higher Rayleigh and Reynolds numbers for other types of cavities and nanofluids.

REFERENCES

[1] D. Poulikakos and A. Bejan, J. Heat Transfer. **105**, 652–655 (1983).
[2] M. Peric, Numer. Heat Transfer, Part A. **24**, 213–219 (1993).
[3] S. H. Tasnim, S. Mahmud and P. K. Das, Int. J. Numer. Methods Heat Fluid Flow. 12 (2002) 855–869.
[4] S. Mahmud, P. K. Das and N. Hyder, Int. Commun. Heat Mass. **29**, 993–1003 (2002).
[5] P. K. Das and S. Mahmud, Int. J. Therm. Sci. **42**, 397–406 (2003).
[6] P. K. Das, S. Mahmud, T. H. Tasnim and A.K.M. S. Islam, Int. J. Numer. Methods Heat Fluid Flow. **13**, 1097–1122 (2003).
[7] C. Biserni, L. A. O. Rocha, G. Stanescu and E. Lorenzini, Int. J. Heat Mass Transfer. **50**, 2132–2138 (2007).
[8] G. Lorenzini, E. D. S. D. Estrada, E. D. dos Santos, L. A. Isoldi and L. A. O. Rocha, Int. J. Heat Mass Transfer. **83**, 75–83 (2015).
[9] Y. Xuan and Q. Li, Int. J. Heat Fluid Flow. **21**, 58–64 (2000).
[10] A. Bejan and M. Almogbel, Int. J. Heat Mass Transfer. **43**, 2101–2115 (2000).
[11] G. Lorenzini, L.A.O. Rocha, Int. J. Heat Mass Transfer. **49**, 4552–4557 (2006).
[12] A. Bejan, Int J. Heat Mass Transfer. **40**, 799–816 (1997).
[13] H. C. Brinkman, J. Chem. Phys. **20**, 571–581 (1952).
[14] J. Maxwell-Garnett, Philos. Trans. Roy. Soc. London Ser. A. **203**, 385–420 (1904).
[15] R. L. Hamilton and O. K. Crosser, Ind. Eng. Chem. Fundamen. **1**, 187–191 (1962).
[16] P. K. Das, X. Li and Z. S. Liu, Appl. Energy **87**, 2785–2796 (2010).
[17] H. F. Oztop and E. Abu-Nada, Int. J. Heat Fluid Flow. **29**, 1326–1336 (2008).